

# New findings for the old problem: Exact solutions for domain walls in coupled real Ginzburg-Landau equations

Boris A. Malomed<sup>1,2</sup>

<sup>1</sup>*Department of Physical Electronics, School of Electrical Engineering,  
Faculty of Engineering, and Center for Light-Matter Interaction,  
Tel Aviv University, P.O. Box 39040 Tel Aviv, Israel*

<sup>2</sup>*Instituto de Alta Investigación, Universidad de Tarapacá, Casilla 7D, Arica, Chile*

This work reports new exact solutions for domain-wall (DW) states produced by a system of coupled real Ginzburg-Landau (GL) equations which model patterns in thermal convection, optics, and Bose-Einstein condensates (BECs). An exact solution for symmetric DW was known for a single value of the cross-interaction coefficient,  $G = 3$  (defined so that its self-interaction counterpart is 1). Here an exact asymmetric DW is obtained for the system in which the diffusion term is absent in one component. It exists for all  $G > 1$ . Also produced is an exact solution for DW in the symmetric real-GL system which includes linear coupling. In addition, an effect of a trapping potential on the DW is considered, which is relevant to the case of BEC. In a system of three GL equations, an exact solution is obtained for a composite state including a two-component DW and a localized state in the third component. Bifurcations which create two lowest composite states are identified too. Lastly, exact solutions are found for the system of real GL equations for counterpropagating waves, which represent a sink or source of the waves, as well as for a system of three equations which includes a standing localized component.

**Keywords:** Rayleigh-Bénard convection; pattern formation; Lyapunov functional; grain boundary; Thomas-Fermi approximation; linear coupling

## I. INTRODUCTION

Complex Ginzburg-Landau (GL) equations is a well-known class of fundamental models underlying the theory of pattern formation under the combined action of linear gain and loss (including diffusion/viscosity), linear wave dispersion, nonlinear loss, and nonlinear dispersion. In the case of the cubic nonlinearity, the generic one-dimensional form of this equation for a complex order parameter,  $u(x, t)$ , is [1, 2]

$$\frac{\partial u}{\partial t} = gu + (a + ib) \frac{\partial^2 u}{\partial x^2} - (d + ic) |u|^2 u. \quad (1)$$

Here, positive constants  $g, d$ , and  $a$  represent, severally, the linear gain, nonlinear loss, and diffusion. Coefficients  $b$  and  $c$ , which may have any sign, control the linear and nonlinear dispersion, respectively. By means of obvious rescaling of  $t, x$ , and  $u$ , one can fix three coefficients in Eq. (1):

$$g = d = a = 1. \quad (2)$$

The ubiquity and great variety of the complex GL equations is illustrated by the title of the well-known review article by Aranson and Kramer [1], *The world of the complex Ginzburg-Landau equation*. These equations are directly derived in settings such as laser cavities, with  $u(x, t)$  being a slowly-varying amplitude of the optical field [3–6]. In many other areas (hydrodynamics, plasmas, chemical waves, etc.), underlying systems of basic equations are more cumbersome, but complex GL equations can be derived as asymptotic ones governing the evolution of long-scale small-amplitude (but, nevertheless, essentially nonlinear) excitations [7–9].

A particular case of Eq. (1) is the real GL equation (in this context, the name had originally appeared from the phenomenological theory of superconductivity elaborated by Ginzburg and Landau 70 years ago [10]):

$$\frac{\partial u}{\partial t} = u + \frac{\partial^2 u}{\partial x^2} - |u|^2 u, \quad (3)$$

which is written with respect to normalization (2). Actually, order parameter  $u(x, t)$  governed by Eq. (3) may be a complex function, while the equation is called “real” because its coefficients are real. The real GL equation is well known as a model of nondispersive nonlinear dissipative media, such as the Rayleigh-Bénard (RB) convection in a layer of a fluid heated from below [11, 12], and instability of a plane laser-driven evaporation front [13].

Unlike Eq. (1) with complex coefficients, real GL equation (3) may be represented in the *gradient form*,  $\partial u/\partial t = -\delta L/\delta u^*$ , where  $\delta/\delta u^*$  stands for the variational (Freché) derivative, and

$$L = \int_{-\infty}^{+\infty} \left( -|u|^2 + \left| \frac{\partial u}{\partial x} \right|^2 + \frac{1}{2}|u|^4 \right) dx \quad (4)$$

is the *Lyapunov functional*. A consequence of the gradient representation is that  $L$  may only decrease or stay constant in the course of the evolution,  $dL/dt \leq 0$ . This fact strongly simplifies dynamics of the real GL equation, especially the study of stability of its stationary solutions.

Equation (3) gives rise to a family of stationary plane-wave (PW) solutions,

$$u(x) = \sqrt{1 - k^2} \exp(ikx), \quad (5)$$

where real wavenumber  $k$  takes values in the existence band,  $-1 < k < +1$ . In terms of the RB convection, the PWs represent the simplest nontrivial patterns in the form of periodic arrays of counter-rotating convective “rolls”, which appear when the Rayleigh number exceeds its critical value [11, 12]. The PW solutions are stable against small perturbations in a part of the existence band, which is selected by the *Eckhaus criterion* [14, 15]:  $-1/\sqrt{3} \leq k \leq +1/\sqrt{3}$ . In the stability subband, the squared amplitude of the PW solution,  $A^2(k)$ , must exceed 2/3 of its maximum value,  $A_{\max}^2 \equiv 1$ , which corresponds to  $k = 0$ :

$$A^2(k) \equiv 1 - k^2 \geq 2/3. \quad (6)$$

The density of the Lyapunov functional (4) of the PW solutions,  $\mathcal{L} = -A^4(k)/2$ , takes values  $\mathcal{L}_{\min} \equiv -1/2 \leq \mathcal{L} \leq (4/9)\mathcal{L}_{\min}$ , as  $k^2$  varies from 0 to 1/3 in the stability interval (6). The presence of the interval of values of  $k$  which give rise to stable roll patterns puts forward the problem of the *wavenumber selection*, which was addressed in various settings [16–19].

In fact, the rolls are quasi-one-dimensional patterns, as the surface of the convection layer is two-dimensional. This fact suggests a possibility of the existence of patterns with linear defects in the form of domain walls (DWs), alias grain boundaries, separating half-infinite areas filled by PWs with wave vectors  $\mathbf{k}_{1,2}$  with different orientations but equal lengths,  $k_{1,2} = 1$ . Such defects may be naturally formed by the Kibble-Zurek mechanism [20, 21], when the switch of the Rayleigh number of the fluid layer heated from below to a supercritical value, at which the convection instability sets in, occurs at two separated spots. They become sources of rolls with independently chosen orientations. Collision between arrays of rolls with different orientation will naturally give rise to an interface in the form of the DW. These structures in the RB convection were predicted theoretically [12, 22–24] and observed in experiments, both as DWs proper and more complex defects, formed by intersecting DWs [25]. Actually, the existence of the DW is a consequence of the effective immiscibility of the PW modes [26, 30] which are separated by the wall.

It is relevant to mention that grain boundaries occur, in a great variety of realizations, as fundamental objects in condensed-matter physics [31–36]. Although the nature of such objects is different from that in the RB convection and other nonlinear dissipative media, the phenomenology of the grain boundaries has many common features in all physical settings where they appear.

DW states were constructed in Ref. [23] as solutions of two coupled real GL equations for amplitudes  $u_1$  and  $u_2$  of PWs connected by the DW, see Eqs. (12) and (13) below. At the level of stationary solutions, the same coupled real equations predict DWs in optics, as boundaries between spatial or temporal domains occupied by PWs representing different polarizations or different wavelengths of light [37, 38]. Further, these equations coincide with the stationary version of the Gross-Pitaevskii (GP) equations which produce DW states in binary Bose-Einstein condensates (BECs) composed of immiscible components [39, 40].

In a particular case, a DW solution of the coupled real GL equations was found in an exact analytical form, see Eq. (15) below. Although the exact solution is not a generic one, it is an obviously important finding, as it provides direct insight into the structure of the respective states. The objective of the present work is to add several new exact solutions of the DW type for more general forms of coupled real GL equations, which exhibit essentially new features. The new solutions are: (i) an exact DW state in the extremely asymmetric system, in which the diffusion coefficient vanishes in one equation; (ii) the system including linear coupling between the components; (iii) a composite state including a DW in two components and a bright soliton in the additional component added to the system; (iv) an exact DW-like state of the *source* or *sink* types in a system of GL equations for counterpropagating waves, which is a basic model for the traveling-wave thermal convection in binary fluids [41–43]. It was known that the interplay of counterpropagating waves could give rise to source and sink modes [44–47], but exact solutions for them were not available. Also reported is an exact composite solution of a system of three equations, in the form of a source or kink formed by two counterpropagating components, coupled to a localized standing mode in the third component. An essential fact is that, unlike the particular exact DW solution originally reported in Ref. [23], which was an isolated

one, with no degrees of freedom, the new solutions reported here appear in *families*, which contain at least one free parameter.

The above-mentioned new exact solutions are presented, respectively, in Sections II – V. In addition, Section III addresses the situation relevant to the realization of the coupled system in BEC, when the GP equations include a trapping harmonic-oscillator (HO) potential. Section IV also reports exact results for bifurcations which create two lowest three-component composite states, with an infinitesimal even or odd mode in the third component, added to the DW. The paper is concluded by Section VI

## II. THE DW (DOMAIN WALL) IN THE ASYMMETRIC SYSTEM

The starting point of the analysis leading to the coupled system of GL equations for slowly-varying amplitudes of  $N$  two-dimensional PWs,  $u_j(x, y, t)$ ,  $j = 1, \dots, N$ , with carrier wave vectors  $\mathbf{k}_j$  of the PWs which form a convection pattern, or a similar one in other physical setups, is the expression for the two-dimensional distribution of the complex order parameter (e.g., the amplitude of the convective flow):

$$U(x, y; t) = \sum_{l=1}^N u_l(x, y; t) \exp(i\mathbf{k}_l \cdot \mathbf{r}), \quad (7)$$

where  $r = (x, y)$  [11, 12, 23]. In the case of  $N = 2$ , the resulting system of coupled one-dimensional GL equations for the configuration which represents the DW oriented along axis  $x$  is, in the scaled form,

$$\frac{\partial u_1}{\partial t} = D_1 \frac{\partial^2 u_1}{\partial x^2} + u_1 \left( 1 - |u_1|^2 - G |u_2|^2 \right), \quad (8)$$

$$\frac{\partial u_2}{\partial t} = D_2 \frac{\partial^2 u_2}{\partial x^2} + u_2 \left( 1 - |u_2|^2 - G |u_1|^2 \right), \quad (9)$$

cf. Eq. (3). Here,  $G > 0$  is the coefficient of the inter-mode interaction, while its counterpart for the self-interaction is scaled to be 1, and diffusion coefficients are

$$D_{1,2} \equiv \cos^2 \theta_{1,2}, \quad (10)$$

where  $\theta_{1,2}$  are angles between vectors  $\mathbf{k}_{1,2}$  and the  $x$  axis. Similar to Eq. (3), this system may be written in the gradient form,  $\partial u_{1,2}/\partial t = -\delta L/\delta u_{1,2}^*$ , with the Lyapunov functional which is an extension of expression (4):

$$L_{12} = \int_{-\infty}^{+\infty} \left[ \sum_{j=1,2} \left( -|u_j|^2 + \left| \frac{\partial u_j}{\partial x} \right|^2 + \frac{1}{2} |u_j|^4 \right) + G |u_1|^2 |u_2|^2 \right] dx. \quad (11)$$

Real DW solutions, interpolating between uniform PW modes  $u_1$  and  $u_2$  at  $x \rightarrow -\infty$  and  $x \rightarrow +\infty$ , respectively, satisfy the stationary version of Eqs. (8) and (9),

$$D_1 \frac{d^2 u_1}{dx^2} + u_1 (1 - u_1^2 - G u_2^2) = 0, \quad (12)$$

$$D_2 \frac{d^2 u_2}{dx^2} + u_2 (1 - u_2^2 - G u_1^2) = 0, \quad (13)$$

and are determined by boundary conditions (b.c.)

$$\begin{aligned} u_1(x \rightarrow -\infty) &= u_2(x \rightarrow +\infty) = 1, \\ u_1(x \rightarrow +\infty) &= u_2(x \rightarrow -\infty) = 0. \end{aligned} \quad (14)$$

These solutions exist under the above-mentioned immiscibility constraints which, in the present notation, is  $G > 1$  (i.e., the inter-component repulsion is stronger than the intrinsic self-repulsion in each component) [26]. If DW solutions to Eqs. (12) and (13) exist, the Lyapunov functional (11) guarantees their stability (it can be checked that they correspond to minima of the functional, rather than to a saddle point).

An essential finding, reported in Ref. [23], is that the symmetric version of Eqs. (12) and (13), with  $D_1 = D_2 \equiv D$ , produces a particular exact solution:

$$G = 3, \left\{ \begin{array}{l} u_1(x) \\ u_2(x) \end{array} \right\} = \frac{1}{2} \left\{ \begin{array}{l} 1 - \tanh\left(\frac{x}{\sqrt{2D}}\right) \\ 1 + \tanh\left(\frac{x}{\sqrt{2D}}\right) \end{array} \right\}. \quad (15)$$

In terms of the BEC realization of Eq. (12) and (13), the single value of the interaction coefficient at which this exact solution is available,  $G = 3$ , can be adjusted by means of the Feshbach-resonance method for binary condensates [27, 28]. In optics, the usual value is  $G = 2$  for the copropagation of waves with orthogonal circular polarizations or different wavelengths, but other values of  $G$  can be adjusted in nonlinear photonic crystals [29].

The first new result, reported here as an essential addition to the well-elaborated theme of DWs, is the fact that it is also possible to find an exact analytical solution in the limit case of the extreme asymmetry in the system of Eqs. (12) and (13), which corresponds to  $D_2 = 0$  and  $D_1 \equiv D > 0$ , i.e., the DW between two roll families one of which has the wave vector perpendicular to the  $x$  axis, see Eq. (10):

$$D \frac{d^2 u_1}{dx^2} + u_1 (1 - u_1^2 - Gu_2^2) = 0, \quad (16)$$

$$u_2 (1 - u_2^2 - Gu_1^2) = 0. \quad (17)$$

Note that the form of Eq. (17), in which the second derivative drops out, corresponds to the well-known Thomas-Fermi (TF) approximation in the BEC theory. In the framework of the TF approximation, the kinetic-energy term in the GP equation is neglected, in comparison with ones representing a trapping potential and the self-repulsive nonlinearity [48]. In the present case,  $D_2 = 0$  is not an approximation, but the exact special case corresponding to  $\theta_2 = 90^\circ$  in Eq. (10). As concerns the application of Eqs. (12) and (13), as a system of stationary GP equations, to BEC, with the kinetic-energy coefficients which are  $D_{1,2} = \hbar^2 / (2m_{1,2})$  in physical units, where  $m_{1,2}$  are atomic masses of the two components of the heteronuclear binary condensate, Eqs. (16) and (17) correspond to a *semi-TF approximation*, representing a mixture of light (small  $m_1$ ) and heavy (large  $m_2$ ) atoms, e.g., a  ${}^7\text{Li}$ - ${}^{87}\text{Rb}$  diatomic gas [49].

Obviously, Eq. (17) yields two solutions, *viz.*, either  $u_2 = 0$ , or one representing the quasi-TF relation,

$$u_2^2(x) = 1 - Gu_1^2(x). \quad (18)$$

Equation (16) with  $u_2 = 0$  yields the usual dark soliton, while the substitution of expression (18) in Eq. (16) may produce a bright-soliton solution. These solutions are matched at a stitch point,

$$x = x_0 \equiv -\sqrt{\frac{D}{2}} \ln \left( \frac{\sqrt{G} + 1}{\sqrt{G} - 1} \right), \quad (19)$$

which is defined by condition  $u_1^2(x) = 1/G$ , according to Eq. (18). The global solution, which complies with b.c. (14), is

$$u_1(x) = \begin{cases} -\tanh \left( x/\sqrt{2D} \right), & \text{at } -\infty < x < x_0, \\ \sqrt{\frac{2}{G+1}} \operatorname{sech} \left[ \sqrt{\frac{G-1}{D}} (x - \xi) \right], & \text{at } x_0 < x < +\infty, \end{cases} \quad (20)$$

$$u_2(x) = \begin{cases} 0, & \text{at } -\infty < x < x_0, \\ \sqrt{1 - Gu_1^2(x)}, & \text{at } x_0 < x < +\infty. \end{cases} \quad (21)$$

Finally, the virtual center of the bright-soliton segment of  $u_1(x)$  is located at

$$x = \xi \equiv x_0 - \sqrt{\frac{D}{G-1}} \ln \left( \sqrt{\frac{2G}{G+1}} + \sqrt{\frac{G-1}{G+1}} \right) \quad (22)$$

(actually, exact solution (20) includes the “tail” of the bright soliton at  $x \geq x_0$ , which does not cover the central point,  $x = \xi$ ). The distance  $x_0 - \xi$ , determined by Eq. (22), defines the effective thickness of the strongly asymmetric DW. Note that, as seen from Eqs. (19) and (20), this exact solution exists under the constraint of  $G > 1$ , which is the above-mentioned immiscibility condition.

It is easy to check that expression (20) satisfies continuity demands for  $u_1(x)$  and  $du_1/dx$  at  $x = x_0$ , and expression (21) provides the continuity of  $u_2(x)$  at the same point. The continuity of  $dx_2/dt$  at  $x = x_0$  is not required, as Eq. (17) does not include derivatives. It is worthy to note that, unlike the above-mentioned exact symmetric solution (15), which exists, as an isolated one, solely at  $G = 3$ , the asymmetric solution given by Eqs. (19)-(22) exists for all values of  $G > 1$ . A typical example of the solution is displayed, for  $D = 1$  and  $G = 2$ , in Fig. 1.

It is relevant to mention that a more complex type of asymmetric DWs was considered, in a numerical form, in Ref. [50]. It is a wall between two uniform bimodal states (square-lattice patterns), built as per Eq. (7), one with a pair of wave vectors corresponding to angles ( $\theta_1 = 0, \theta_2 = \pi/2$ ), and the other pair rotated by  $\pi/4$ , i.e., with  $\theta_{1,2} = \pm\pi/4$ .

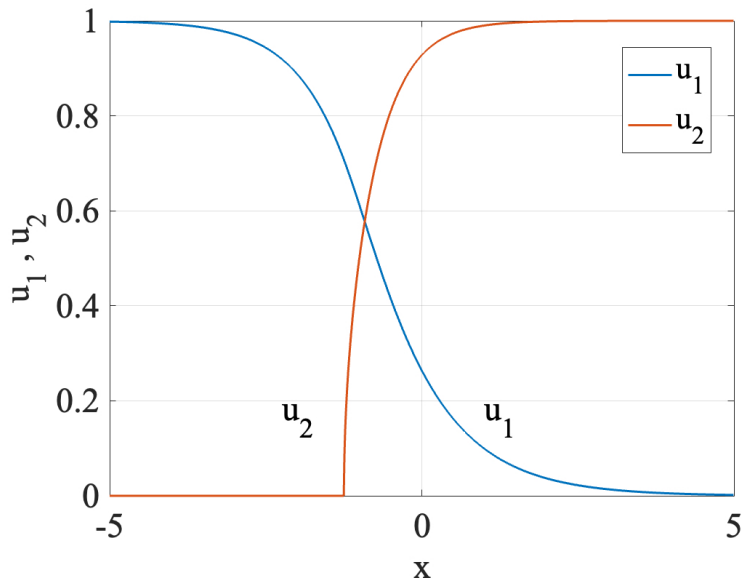


FIG. 1. An example of the asymmetric DW, as given by Eqs. (19)-(22), for  $D = 1$  and  $G = 2$ . Note that the coordinate of the stitch point is, in this case,  $x_0 \approx -1.25$ , as per Eq. (19), and the “virtual center” of the bright-soliton segment of  $u_1(x)$  is located at  $\xi \approx -1.80$ , as per Eq. (22).

### III. THE DW IN THE SYMMETRIC SYSTEM WITH LINEAR COUPLING, AND THE EFFECT OF THE TRAPPING POTENTIAL

#### A. The exact solution

The system of Eqs. (12) and (13), as it appears in above-mentioned realizations in optics and BEC, may also include linear mixing between the components. In particular, this effect is produced by twist applied to a bulk optical waveguide [51, 52]. A similar effect in binary BEC, *viz.*, mutual inter-conversion of two atomic states, which form the binary condensate, may be induced by the resonant radio-frequency field [54]. The respectively modified symmetric system of Eqs. (12) and (13) is

$$D \frac{d^2 u_1}{dx^2} + u_1 (1 - u_1^2 - G u_2^2) + \lambda u_2 = 0, \quad (23)$$

$$D \frac{d^2 u_2}{dx^2} + u_2 (1 - u_2^2 - G u_1^2) + \lambda u_1 = 0, \quad (24)$$

where real  $\lambda$  is the linear-coupling coefficient. In fact, Eqs. (23) and (24) apply to the RB convection too, in the case when periodic corrugation of the bottom of the convection cell, with amplitude  $\sim \lambda$  and wave vector  $\mathbf{k}_1 + \mathbf{k}_2$  (see Eq. (7)), gives rise to the *linear cross-gain*, which is used in many laser setups that are similar to thermal convection [57, 58].

The system of Eqs. (23) and (24) with  $G = 3$  admits an exact DW solution, which is an extension of its counterpart (15):

$$\begin{cases} u_1(x) \\ u_2(x) \end{cases} = \frac{1}{2} \begin{cases} \sqrt{1+\lambda} - \sqrt{1-\lambda} \tanh \left( \sqrt{\frac{1-\lambda}{2D}} x \right) \\ \sqrt{1+\lambda} + \sqrt{1-\lambda} \tanh \left( \sqrt{\frac{1-\lambda}{2D}} x \right) \end{cases}. \quad (25)$$

Due to the action of the linear mixing, b.c. (14) are replaced by

$$\begin{aligned} u_1(x \rightarrow -\infty) &= u_2(x \rightarrow +\infty) = \frac{1}{2} (\sqrt{1+\lambda} + \sqrt{1-\lambda}), \\ u_1(x \rightarrow +\infty) &= u_2(x \rightarrow -\infty) = \frac{1}{2} (\sqrt{1+\lambda} - \sqrt{1-\lambda}). \end{aligned} \quad (26)$$

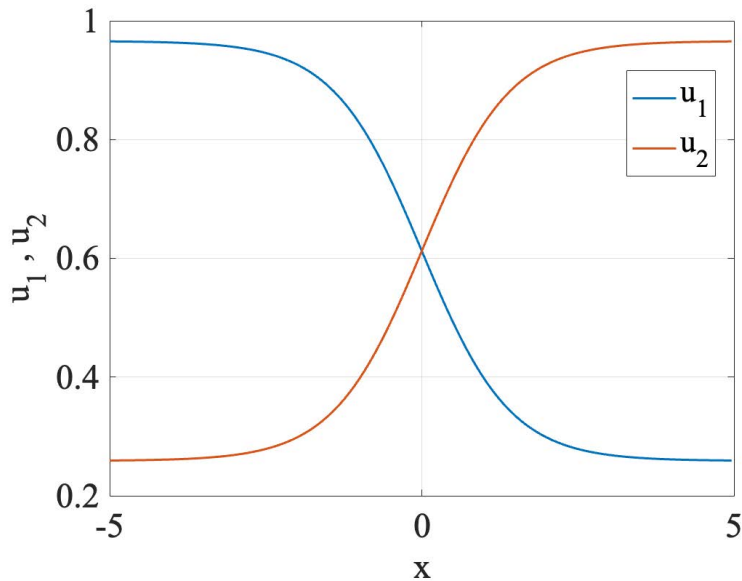


FIG. 2. An example of the symmetric DW in the presence of the linear coupling, as given by Eqs. (25) and (26), for  $D = \lambda = 1/2$ . Note that the asymptotic values of the components at  $x \rightarrow \pm\infty$ , as given by Eqs. (26) are, in this case,  $u_1(x \rightarrow -\infty) = u_2(x \rightarrow +\infty) \approx 0.97$  and  $u_1(x \rightarrow +\infty) = u_2(x \rightarrow -\infty) \approx 0.26$ .

These solutions exist for all values of  $0 \leq \lambda < 1$ . A typical example is displayed in Fig. 2.

### B. Effects of the trapping potential

The realization of the system in terms of the binary BEC should include, generally speaking, the trapping HO potential, which is normally used in the experiment [48]. The accordingly modified system of Eqs. (23) and (24) is

$$D \frac{d^2 r_1}{dx^2} + r_1 (1 - r_1^2 - Gr_2^2) + \lambda r_2 = \frac{\aleph^2}{2} x^2 r_1, \quad (27)$$

$$D \frac{d^2 r_2}{dx^2} + r_2 (1 - r_2^2 - Gr_1^2) + \lambda r_1 = \frac{\aleph^2}{2} x^2 r_2, \quad (28)$$

where  $\aleph^2$  is the strength of the OH potential. DW solutions of the system of Eqs. (27) and (28) were addressed in Ref. [55]. In the absence of the linear coupling ( $\lambda = 0$ ), a rigorous mathematical framework for the analysis of such solutions was elaborated in Ref. [56].

If the HO trap is weak, *viz.*,  $\aleph^2 \ll 4/(1 - \lambda)$ , the DW solution trapped in the OH potential takes nearly constant values, close to those in Eq. (26), in the region of

$$2D/(1 - \lambda) \ll x^2 \ll 8D/\aleph^2. \quad (29)$$

On the other hand, at  $x^2 \rightarrow \infty$  solutions generated by Eqs. (27) and (28) decay similar to eigenfunctions of the HO potential in quantum mechanics, *viz.*,

$$r_{1,2} \approx \varrho_{1,2} |x|^\gamma \exp\left(-\frac{\aleph}{2\sqrt{2D}} x^2\right), \quad (30)$$

$$\gamma = \frac{1 + \lambda}{\sqrt{2D}\aleph} - \frac{1}{2}, \quad (31)$$

where  $\varrho_{1,2}$  are constants. In the case of  $\lambda = 0$ , the asymptotic tails (30) follow the structure of solution (15), i.e.,  $\varrho_1(x \rightarrow +\infty) = \varrho_2(x \rightarrow -\infty) = 0$  and  $\varrho_1(x \rightarrow -\infty) = \varrho_2(x \rightarrow +\infty) \neq 0$ . On the other hand, the linear mixing,  $\lambda \neq 0$ , makes the tail symmetric with respect to the two components, with  $\varrho_1(|x| \rightarrow \infty) = \varrho_2(|x| \rightarrow \infty) \neq 0$ . Note that  $\gamma = 0$  in Eq. (31) with  $\lambda = 0$  is tantamount to the case when values of  $\aleph$  and  $D$  in Eqs. (27) and (28) correspond to the ground state of the HO potential.

## IV. DW-BRIGHT-SOLITON COMPLEXES

### A. An exact solution for the composite state

The DW formed by two immiscible PWs may serve as an effective potential for trapping an additional PW mode. To address this possibility, it is relevant to consider the symmetric configuration, with  $D_1 = D_2 \equiv D$  (see Eq. (10)), and wave vector  $\mathbf{k}_v$  of the additional PW mode,  $v(x)$ , directed along the bisectrix of the angle between the DW-forming wave vectors  $\mathbf{k}_1$  and  $\mathbf{k}_2$ , i.e., along axis  $x$  (hence Eq. (10) yields  $D_v = 1$ ). The corresponding system of three coupled stationary real GL equations is

$$D \frac{d^2 u_1}{dx^2} + u_1 (1 - u_1^2 - Gu_2^2 - gv^2) = 0, \quad (32)$$

$$D \frac{d^2 u_2}{dx^2} + u_2 (1 - u_2^2 - Gu_1^2 - gv^2) = 0, \quad (33)$$

$$\frac{d^2 v}{dx^2} + (1 - v^3 - g(u_1^2 + u_2^2))v = 0, \quad (34)$$

where  $g > 0$  is the constant of the nonlinear interaction between components  $u_{1,2}$  and  $v$ .

The system of Eqs. (32)-(34) admits the following exact solution, in the form of the DW of components  $u_{1,2}(x)$  coupled to a bright-soliton profile of  $v(x)$ :

$$\begin{Bmatrix} u_1(x) \\ u_2(x) \end{Bmatrix} = \frac{1}{2} \begin{Bmatrix} 1 - \tanh(\sqrt{g-1}x) \\ 1 + \tanh(\sqrt{g-1}x) \end{Bmatrix}, \quad (35)$$

$$v(x) = \sqrt{2 - \frac{3}{2}g} \operatorname{sech}(\sqrt{g-1}x). \quad (36)$$

This solution is valid under the condition that coefficients  $G$  and  $D$  in Eqs. (32) and (33) take the following particular values,

$$G = 3 - 8g + 6g^2, \quad (37)$$

$$D = \frac{1}{2}(3g - 1). \quad (38)$$

As is follows from Eq. (36),  $g$  is a free parameter of this solution, which may take values in a narrow interval,

$$1 < g < 4/3 \quad (39)$$

(see also Eq. (45) below). According to Eqs. (37) and (38), the interval (39) of the variation of  $g$  corresponds to coefficients  $G$  and  $D$  varying in intervals

$$1 < G < 3; \quad 1 < D < 3/2. \quad (40)$$

Thus, adding the  $v$  component lifts the degeneracy of the exact DW solution (15), which exists solely at  $G = 3$ .

Recall that, in the model of convection patterns, coefficient  $D$ , as given by Eq. (10), cannot take values  $D > 1$ , which disagrees with Eq. (40). However, values  $D > 1$  are relevant for systems of GP equations for the heteronuclear three-component BEC. In the latter case,  $D$  is the ratio of atomic masses of the different species which form the triple immiscible BEC. Similarly,  $D$  is the ratio of values of the normal group-velocity dispersion of copropagating waves in the temporal-domain realization of the real GL equations in nonlinear fiber optics [37].

An example of the DW-bright-soliton complex is displayed in Fig. 3 for  $g = 7/6$ , in which case Eqs. (37) and (38) yield  $G = 11/6$  and  $D = 5/4$  (according to Eqs. (37) and (10)). The fact that the respective soliton's amplitude, which is  $\sqrt{2 - 3g/2} = 1/2$  according to Eq. (36), coincides with the mid value of the DW components (35), is a peculiarity of this particular case.

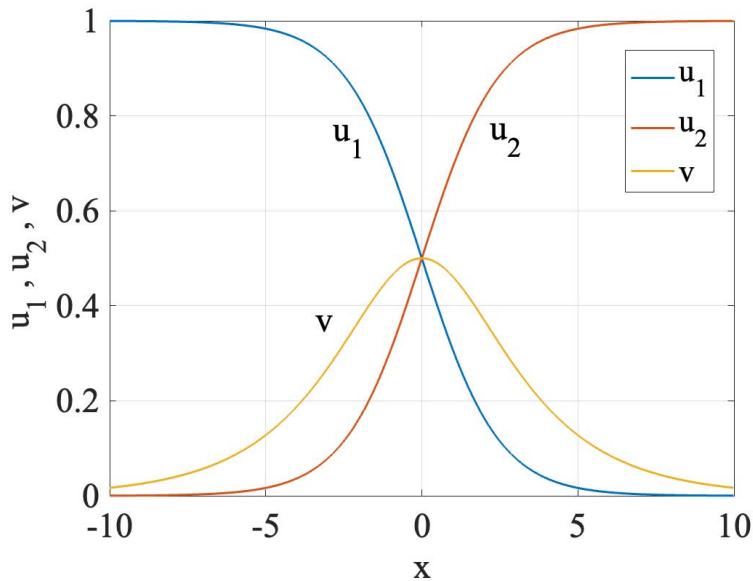


FIG. 3. An example of the exact solution for the DW-bright-soliton complex, given by Eqs. (35) and (36), for  $g = 7/6$ ,  $G = 11/6$ , and  $D = 5/4$ .

### B. The bifurcation of the creation of the composite state in the general case

If relation (37) is not imposed on the interaction coefficients  $g$  and  $G$ , the solution for the composite state cannot be found in an exact form. Nevertheless, it is possible to identify *bifurcation points* at which component  $v$  with an infinitesimal amplitude appears. To this end, Eq. (34) should be used in the form linearized with respect to  $v$ :

$$\frac{d^2v}{dx^2} + \{1 - g[u_1^2(x) + u_2^2(x)]\}v = 0. \quad (41)$$

This linear equation can be exactly solved for  $u_1(x) = u_2(x)$  given by expression (15), in the case of  $G = 3$ , while parameters  $D$  and  $g$  may take arbitrary values. Indeed, using the commonly known results for the Pöschl-Teller potential in quantum mechanics, it is easy to find that Eq. (41) with the effective potential corresponding to Eq. (15) gives rise to spatially even eigenmodes in the form of

$$v(x) = \text{const} \cdot \left[ \text{sech} \left( x/\sqrt{2D} \right) \right]^\alpha, \quad (42)$$

at a special value of the interaction coefficient, which identifies the bifurcation producing the composite state:

$$g_{\text{bif}} = D^{-1} \left( 1 + 2D \mp \sqrt{1 + 2D} \right), \quad (43)$$

the respective value of power  $\alpha$  in expression (42) being

$$\alpha = \sqrt{2 \left( 1 + D \mp \sqrt{1 + 2D} \right)}. \quad (44)$$

The values given by Eqs. (43) and (44) with the top sign from  $\mp$  correspond to the bifurcation creating a fundamental composite state (the ground state, in terms of the quantum-mechanical analog) at  $g > g_{\text{bif}}$ , while the bottom sign represents a higher-order bifurcation (alias the second excited state, in the language of quantum mechanics; the first excited state, is a spatially odd mode which is considered below). While it is obvious that the fundamental bifurcation creates a stable composite state, the ones produced by higher-order bifurcations may be unstable.

Further, varying coefficient  $D$  of the modes forming the underlying DW between  $D = 0$  and  $D = \infty$  (recall that the convection model corresponds to  $D < 1$ , while the realizations in optics and BEC admit  $D > 1$ ), Eq. (43) demonstrates monotonous variation of the bifurcation point in interval

$$g_{\text{bif}}(D = 0) \equiv 1 < g_{\text{bif}} < 2 \equiv g_{\text{bif}}(D \rightarrow \infty). \quad (45)$$

It extends interval (39) in which exact composite states with a finite amplitude were found above, see Eqs. (35)-(38).

An odd linear mode produced by Eq. (41) with  $u_{1,2}(x)$  taken from Eq. (15) is looked for as

$$v(x) = \text{const} \cdot \sinh\left(x/\sqrt{2D}\right) \left[\text{sech}\left(x/\sqrt{2D}\right)\right]^\beta. \quad (46)$$

The corresponding exact solution for the quantum-mechanical Pöschl-Teller potential has

$$\beta = \sqrt{2D\left(g_{\text{bif}}^{(\beta)} - 1\right)} + 1 \equiv 1 + \sqrt{2\left(D + 7 - 3\sqrt{2D + 5}\right)}, \quad (47)$$

$$g_{\text{bif}}^{(\text{odd})} = D^{-1}\left(2D + 7 - 3\sqrt{2D + 5}\right). \quad (48)$$

This solution is valid for  $D > 2$ . As  $D$  varies from 2 to  $\infty$ , expression (48) monotonously increases from  $g_{\text{bif}}^{(\text{odd})} = 1$  to  $g_{\text{bif}}^{(\text{odd})} = 2$ . Note that, at  $D = 2$ , Eq. (43) yields  $g_{\text{bif}}(D = 2) = (1/2)(5 - \sqrt{5}) \approx 1.382$ . Actually, at all values of  $D \geq 2$ , the value of  $g_{\text{bif}}^{(\text{odd})}$  is *smaller* than  $g_{\text{bif}}$ , which is given by Eq. (43) for the fundamental (even) mode. This fact implies that, with the increase of  $g$ , the bifurcation creating the spatially odd mode in the  $v$  component happens *earlier* than the bifurcation which creates the even mode.

At  $D = 2$ , Eq. (47) yields  $\beta = 1$ , which corresponds to the delocalized eigenmode (46),  $v(x) = \text{const} \cdot \tanh\left(x/\sqrt{2D}\right)$ . With the increase of  $D$ ,  $\beta$  increases monotonously towards  $\beta \rightarrow \infty$ .

## V. DOMAIN WALLS BETWEEN TRAVELING WAVES

### A. The sink and source in the two-component system

In the simplest case, the system of GL equations for counterpropagating dissipative waves can be written in the form which neglects dispersive effects but includes the opposite group velocities,  $\pm c$  [46]:

$$\frac{\partial u_1}{\partial t} + c \frac{\partial u_1}{\partial x} = u_1 + \frac{\partial^2 u_1}{\partial x^2} - u_1(|u_1|^2 + G|u_2|^2), \quad (49)$$

$$\frac{\partial u_2}{\partial t} - c \frac{\partial u_2}{\partial x} = u_2 + \frac{\partial^2 u_2}{\partial x^2} - u_2(|u_2|^2 + G|u_1|^2). \quad (50)$$

These equations, unlike Eqs. (8) and (9), do not admit the gradient representation. Nevertheless, the stationary form of Eqs. (49) and (50) amounts to real equations:

$$+c \frac{du_1}{dx} = \frac{d^2 u_1}{dx^2} + u_1(1 - u_1^2 - Gu_2^2), \quad (51)$$

$$-c \frac{du_2}{dx} = \frac{d^2 u_2}{dx^2} + u_2(1 - u_2^2 - Gu_1^2). \quad (52)$$

In this case, the relevant b.c. keeps the form of Eq. (14).

An exact solution to Eqs. (51) and (52) can be found following the pattern of Eq. (15):

$$\begin{cases} u_1(x) \\ u_2(x) \end{cases} = \frac{1}{2} \begin{cases} 1 - \tanh\left(\left(\sqrt{8 + c^2} + c\right)(x/4)\right) \\ 1 + \tanh\left(\left(\sqrt{8 + c^2} + c\right)(x/4)\right) \end{cases}, \quad (53)$$

in the case when the cross-interaction coefficient takes a specific value

$$G - 3 = c\left(\sqrt{8 + c^2} + c\right), \quad (54)$$

or, inversely,

$$c = (G - 3)/\sqrt{2(G + 1)}. \quad (55)$$

Thus, this solution lifts the degeneracy of the ‘‘old’’ one (15), which exists solely at  $G = 3$ . Further, it follows from Eq. (54) and (34) that  $\text{sgn}(v) = \text{sgn}(G - 3)$ , hence, taking into regard b.c. (14), one concludes that the exact solution (53) represents a *sink* of traveling waves ( $c > 0$ ) for  $G > 3$ , and a *source* ( $c < 0$ ) for  $G < 3$ . Typical examples of the sink and source are displayed in Figs. 4(a) and (b), respectively. The solution of the latter type exists even in the

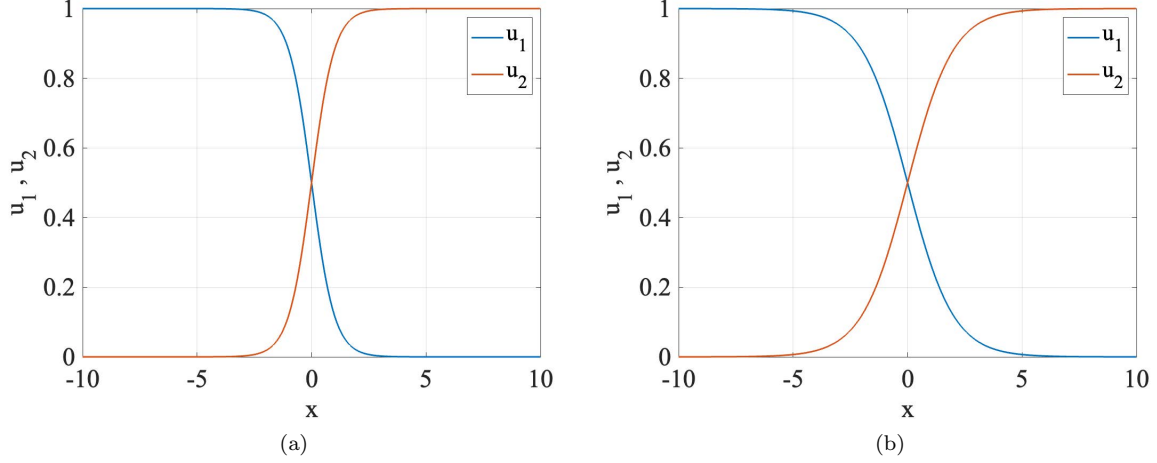


FIG. 4. Examples of the exact stationary solution for coupled traveling waves, given by Eq. (53): (a) a *sink*, for  $G = 7$  and  $c = +1$  in Eqs. (51) and (52); (b) a *source*, for  $G = 1$  and  $c = -1$ .

case of  $G < 1$ , when the two components are miscible; in that case, the separation between them in the DW pattern is maintained by the opposite group velocities, which pull the components apart, preventing the onset of the mixing. In fact, it follows from Eq. (55) that the solution persists even in the range of moderately strong *attraction* between the component,  $-1 < G < 0$ . Note that the pressure of the incoming stationary flows makes the sink mode in Fig. 4(a) conspicuously narrower than its source counterpart drawn in Fig. 4(b) for the same absolute value of the group velocities,  $|c| = 1$ . The source is broader as it is stretched by the egressing flows, even if it is plotted for much weaker mutual repulsion between the components ( $G = 1$ ) than the sink, which pertains to  $G = 7$ .

### B. The composite state in the three-component system

The pair of counterpropagating traveling waves which can trap the additional standing one are described by the following generalization of Eqs. (51) and (52):

$$+c \frac{du_1}{dx} = \frac{d^2u_1}{dx^2} + u_1 (1 - u_1^2 - Gu_2^2 - gv^2), \quad (56)$$

$$-c \frac{du_2}{dx} = \frac{d^2u_2}{dx^2} + u_2 (1 - u_2^2 - Gu_1^2 - gv^2), \quad (57)$$

to which an equation for the standing mode is added, cf. Eq. (34):

$$\frac{d^2v}{dx^2} + (1 - v^2 - g(u_1^2 + u_2^2))v = 0, \quad (58)$$

An exact solution of Eqs. (56)-(58) can be found for free parameters  $g$  and  $c$ :

$$u_{1,2}(x) = \frac{1}{2} \left( 1 \mp \tanh \left( \sqrt{g-1}x \right) \right), \quad (59)$$

$$v(x) = \sqrt{2 - \frac{3}{2}g} \operatorname{sech} \left( \sqrt{g-1}x \right), \quad (60)$$

$$G - 3 = 2g(3g - 4) + 4c\sqrt{g-1}, \quad (61)$$

$$D = \frac{c}{2\sqrt{g-1}} + \frac{1}{2}(3g - 1), \quad (62)$$

cf. Eqs. (35)-(38). As it is seen from Eq. (61), the interaction with the soliton-shaped standing wave shifts the boundary between the sink and source of the traveling waves from the above-mentioned point,  $G = 3$ .

Further, if, in the absence of  $v(x)$ , the bimodal solution for traveling waves is given by Eqs. (53)-(55), the consideration of the bifurcation which gives rise to infinitesimal even and odd modes in the  $v$  component produces the same results as given above, respectively, by Eqs. (42)-(44) and (46)-(48), with  $D$  replaced by

$$D_{\text{eff}} = \frac{8D^2}{(c + \sqrt{c^2 + 8D})^2} \quad (63)$$

(note that, in the limit of  $D \rightarrow \infty$ , Eq. (63) yields  $D_{\text{eff}} \approx D$ ). In particular, the value of  $D = 2$ , at which the odd modes appears above, is replaced by  $D_{\text{eff}} = 2$ , which corresponds to  $D = 2 + c$ .

## VI. CONCLUSION

The aim of this paper is to report new exact solutions for the well-known problem of constructing DW (domain-wall) solutions of the system of coupled real GL (Ginzburg-Landau) equations. These equations apply to modeling DW patterns (alias grain boundaries) in RB (Rayleigh-Bénard) convection, nonlinear optics, and binary BEC. Even if exact solutions cannot be generic ones, particular analytical solutions are quite useful, as they provide direct insight into the structure of DW states. A particular exact solution for the symmetric DW was found long ago in Ref. [23]. It is an isolated solution, which exists at the single value of the cross-interaction coefficient,  $G = 3$ . In this work, first, an exact solution for strongly asymmetric DWs is found in the form of Eqs. (19)-(22), for the system in which the diffusion term is present in one component only. Unlike the “old” exact solution for the symmetric DW, the newly found one is available at all values of  $G > 1$ , which is the fundamental condition for immiscibility of the two components. An exact solution for the symmetric DW, in the system including the linear coupling between the components, is found too, given by Eq. (25). In addition to that, the effect of the trapping harmonic-oscillator potential on the DW is considered, leading to the asymptotic form of the solution presented by Eqs. (30) and (31). Another essential finding is exact solution (32)-(34) for the system of three coupled GL equations for a composite state built of a symmetric DW between two components and a bright soliton in the third one. This solution also lifts the degeneracy of the “old” one, fixed by  $G = 3$ . In addition to this result, the location of the bifurcations, which create the composite states from the two-component DW, are found in the exact form, as given by Eqs. (42)-(44) or (46)-(48) for the bifurcations creating, respectively, the spatially even (fundamental) or odd component in the third component. The stability of all these exact solutions is provided by the gradient structure of the underlying systems of time-dependent GL equations. Finally, another exact stationary solution, provided by Eqs. (53)-(55), is generated by the system of GL equations governing the interaction of counterpropagating waves with opposite group velocities. The solution also lifts the degeneracy condition  $G = 3$  and, depending on the sign of  $G - 3$ , it represents either a sink or source of the waves. The source-type states exists even in the case of  $G < 1$ , when the immiscibility condition does not hold for the interacting components. The latter solution is complemented by the exact composite one, given by Eqs. (59)-(62), which includes the localized mode in the third (standing) component. The respective bifurcations are identified too, by means of Eq. (63).

As an extension of this work, it may be relevant to develop the analysis for families of generic DW states originating from the particular exact solutions reported in this paper. This can be done by means of the perturbation theory and numerical methods.

## ACKNOWLEDGMENTS

I thank Michael Tribelsky, Alexander Nepomnyashchy, and Dmitry Pelinovsky for valuable discussions. The help of Zhaopin Chen in producing plots included in this paper is highly appreciated. This work was supported, in part, by Israel Science Foundation through grant No. 1286/17.

- 
- [1] I. S. Aranson, L. Kramer, The world of the complex Ginzburg-Landau equation, *Rev. Mod. Phys.* **74** (2002) 99-143.
  - [2] B. A. Malomed, Complex Ginzburg-Landau equation. In: *Encyclopedia of Nonlinear Science*, pp. 157-160. A. Scott, editor (Routledge, New York, 2005).
  - [3] F. T. Arecchi, S. Boccaletti, P. Ramazza, Pattern formation and competition in nonlinear optics, *Phys. Rep.* **318**, 1–83 (1999).
  - [4] N. N. Rosanov, Transverse patterns in wide-aperture nonlinear optical systems, *Progr. Opt.* **35**, 1-60 (1996).
  - [5] N. N. Rosanov, *Spatial Hysteresis and Optical Patterns* (Springer-Verlag, Berlin, 2002).

- [6] M. Inc, A. I. Aliyu, A. Yusuf, D. Baleanu, Optical solitons for complex Ginzburg-Landau model in nonlinear optics, *Optik* **158** (2018) 368-375.
- [7] M. C. Cross, P. C. Hohenberg, Pattern-formation outside of equilibrium, *Rev. Mod. Phys.* **65**, 851-1112 (1993).
- [8] M. Ipsen, L. Kramer, P. G. Sorensen. Amplitude equations for description of chemical reaction-diffusion systems, *Phys. Rep.* **337**, 193-235 (2000).
- [9] R. Hoyle, *Pattern Formation: An Introduction to Methods* (Cambridge University Press, Cambridge, 2006).
- [10] V. L. Ginzburg, L. D. Landau, On the theory of superconductivity, *Zhurnal Eksperimentalnoy i Teoreticheskoy Fiziki* (USSR), **20**, 1064-1082 (1950) (in Russian) [English translation: in *Men of Physics*, vol. 1. Oxford: Pergamon Press, 1965. pp. 138-167].
- [11] F. H. Busse, The stability of finite amplitude cellular convection and its relation to an extremum principle. *J. Fluid Mech.* **30**, 625-649 (1967).
- [12] M. C. Cross, Ingredients of a theory of convective textures close to onset, *Phys. Rev. A* **25** (1982) 1065-1076.
- [13] S. I. Anisimov, M. I. Tribelsky, Y. G. Epelbaum, Instability of a plane evaporation boundary in the interaction between laser radiation and matter, *Zh. Eksp. Teor. Fiz. [Sov. Phys. JETP]* **78** (1980) 1597-1605.
- [14] W. Eckhaus, *Studies in Non-Linear Stability Theory* (Springer, New York, 1965).
- [15] B. A. Malomed, M. I. Tribelsky, Bifurcations in distributed kinetic systems with aperiodic instability, *Physica D* **14** (1984) 67-87.
- [16] L. Kramer, E. Ben-Jacob, H. Brand, *Phys. Rev. Lett.* **49** (1982) 1891.
- [17] A. A. Nepomnyashchy, M. I. Tribelsky, M. G. Velarde, *Phys. Rev. E* **50** (1994) 1194-1197.
- [18] M. van Hecke, C. Storm, and W. van Saarloos, Sources, sinks and wavenumber selection in coupled CGL equations and experimental implications for counter-propagating wave systems, *Physica D* **134** (1999) 1-47.
- [19] M. Haragus, A. Scheel, Grain boundaries in the Swift-Hohenberg equation, *Eur. J. Appl. Math.* **23** (2012) 737-759.
- [20] S. Casado, W. Gonzalez-Vinas, H. Mancini, Testing the Kibble-Zurek mechanism in Rayleigh-Bénard convection, *Phys. Rev. E* **74** (2006) 047101.
- [21] M. A. Miranda, D. Laroze, W. Gonzalez-Vinas, The Kibble-Zurek mechanism in a subcritical bifurcation, *J. Phys. Cond. Matt.* **25** (2013) 404208.
- [22] P. Manneville, Y. Pomeau, A grain-boundary in cellular structures near the onset of convection. *Phil. Mag. A* **48** (1983) 607-621.
- [23] B. A. Malomed, A. A. Nepomnyashchy, M. I. Tribelsky, Domain boundaries in convection patterns. *Phys. Rev. A* **42** (1990) 7244-7263.
- [24] M. Haragus, G. Iooss, Bifurcation of symmetric domain walls for the Bénard-Rayleigh convection problem. *Arch. Rational Mech. Anal.* **239** (2021) 733-781.
- [25] V. Steinberg, G. Ahlers, D. S. Cannell, Pattern formation and wave-number selection by Rayleigh-Bénard convection in a cylindrical container, *Physica Scripta* **32** (1985) 534-547.
- [26] V. P. Mineev, The theory of the solution of two near-ideal Bose gases. *Zh. Eksp. Teor. Fiz.* **67** (1974) 263-272 (1974) [English translation: *Sov. Phys. - JETP* **40** (1974) 132-136].
- [27] R. Grimm, P. Julienne, E. Tiesinga, Feshbach resonances in ultracold gases, *Rev. Mod. Phys.* **82** (2010) 1225-1286.
- [28] F. Wang, X. Li, D. Xiong, D. Wang, A double species  $^{23}\text{Na}$  and  $^{87}\text{Rb}$  Bose-Einstein condensate with tunable miscibility via an interspecies Feshbach resonance. *J. Phys. B: At. Mol. Opt. Phys.* **49** (2016) 015302.
- [29] M. Skorobogatiy, J. Yang, *Fundamentals of Photonic Crystal Guiding* (Cambridge University Press, Cambridge, 2009).
- [30] M. E. Gurtin, D. Polignone, J. Vinals, Two-phase binary fluids and immiscible fluids described by an order parameter, *Math. Models & Methods in Appl. Sci.* **6** (1996) 815-831.
- [31] G. S. Rohrer, Grain boundary energy anisotropy: a review, *J. Materials Science*, **46** (2011) 5881-5895.
- [32] H. Lim, M. G. Lee, R. H. Wagoner, Simulation of polycrystal deformation with grain and grain boundary effects, *Int. J. Plasticity* **27** (2011) 1328-1354.
- [33] P. Rudolph, Dislocation patterning and bunching in crystals and epitaxial layers - a review, *Cryst. Res. Tech.* **52** (2017) 1600171.
- [34] U. Atxitia, D. Hinzke, U. Nowak, Fundamentals and applications of the Landau-Lifshitz-Bloch equation, *J. Phys. D: Appl. Phys.* **50** (2017) 033003.
- [35] E. G. Galkina, B. A. Ivanov. Dynamic solitons in antiferromagnets, *Low Temp. Phys.* **44** (2018) 618-633.
- [36] W. Yao, B. Wu, Y. Liu, Growth and grain boundaries in 2D materials, *ACS Nano* **14** (2020) 9320-9346.
- [37] B. A. Malomed, Optical domain walls, *Phys. Rev. E*, **50** (1994) 1565-1571.
- [38] Y. F. Song, X. J. Shi, C. F. Wu, D. Y. Tang, H. Zhang, Recent progress of study on optical solitons in fiber lasers, *Appl. Phys. Rev.* **6** (2019) 021313.
- [39] M. Trippenbach, K. Góral, K. Rzażewski, B. Malomed, Y. B. Band, Structure of binary Bose-Einstein condensates, *J. Phys. B: At. Mol. Opt. Phys.* **33**, (2000) 4017-4031.
- [40] P. G. Kevrekidis, H. E. Nistazakis, D. J. Frantzeskakis, B. A. Malomed, R. Carretero-González, Families of matter-waves in two-component Bose-Einstein condensates, *Eur. Phys. J. D* **28** (2004), 181-185.
- [41] Cross, M. C. Traveling and standing waves in binary-fluid convection in finite geometries. *Phys. Rev. Lett.* **1986**, 57, 2935-2938.
- [42] Cross, M. C. Structure of nonlinear traveling-wave states in finite geometries, *Phys. Rev. A* **1988**, 38, 3593-3600 (1988).
- [43] Voss, H. U.; Kolodner, P.; Abel, M.; Kurths, J. Amplitude equations from spatiotemporal binary-fluid convection data. *Phys. Rev. Lett.* **1999**, 83, 3422-3425.
- [44] Y. Pomeau, Front motion, metastability and subcritical bifurcations in hydrodynamics, *Physica D* **23** (1986) 3-11.

- [45] P. Coulet, T. Frisch, F. Plaza, Sources and sinks of wave patterns, *Physica D* **62** (1993) 75-79.
- [46] B. A. Malomed, Domain wall between traveling waves, *Phys. Rev. E* **50** (1994) R3310-R3313.
- [47] B. A. Malomed, Stability and grain boundaries in the dispersive Newell-Whitehead-Siegel equation, *Physica Scripta* **57** (1997) 115-117.
- [48] L. P. Pitaevskii, S. Stringari, *Bose-Einstein Condensation* (Oxford University Press, Oxford, 2003).
- [49] C. Marzok, B. Deh, P. W. Courteille, C. Zimmermann, Ultracold thermalization of  $^7\text{Li}$  and  $^{87}\text{Rb}$ , *Phys. Rev. A* **76** (2000) 052704.
- [50] H. Rotstein and B. A. Malomed, A quasicrystalline domain wall in nonlinear dissipative patterns, *Physica Scripta* **62** (2000) 164-168.
- [51] S. Longhi, Wave packet dynamics in a helical optical waveguide, *Phys. Rev. A* **71** (2005) 055402.
- [52] D. Van Orden, Y. Fainman, V. Lomakin, Twisted chains of resonant particles: optical polarization control, waveguidance, and radiation, *Opt. Lett.* **35** (2010) 2579-2581.
- [53] Y. S. Kivshar, G. P. Agrawal. *Optical Solitons: From Fibers to Photonic Crystals* (Academic Press, San Diego, 2003).
- [54] R. J. Ballagh, K. Burnett, T. F. Scott, Theory of an output coupler for Bose-Einstein condensed atoms, *Phys. Rev. Lett.* **78** (1997) 1608-1611.
- [55] M. I. Merhasin, B. A. Malomed, R. Driben, Transition to miscibility in a binary Bose-Einstein condensate induced by linear coupling, *J. Phys. B: At. Mol. Opt. Phys.* **38** (2005) 877-892.
- [56] S. Alama, L. Bronsard, A. Contreras, D. E. Pelinovsky, Domain walls in the coupled Gross-Pitaevskii equations, *Arch. Rat. Mech. Appl.* **215** (2015) 579-615.
- [57] M. Asghari, I. H. White, R. V. Penty, Wavelength conversion using semiconductor optical amplifiers, *J. Lightwave Tech.* **15** (1997) R3310-R3313.
- [58] J. Kim, M. Laemmlin, C. Meuer, D. Bimberg, G. Eisenstein, Theoretical and experimental study of high-speed small-signal cross-gain modulation of quantum-dot semiconductor optical amplifiers. *IEEE J. Quant. Elect.* **45** (2009) 240-248.